Directional Delay Spread and Interference Quotient Analysis in sub-7GHz Wi-Fi bands

Jorge Gomez-Ponce*†, Daoud Burghal*, Naveed A. Abbasi*
Arjun Hariharan*, Gopal Jakhetia*, Praveen Chaganlal*, Andreas F. Molisch*
*University of Southern California, Los Angeles, CA, USA
Email: {gomezpon, burghal, nabbasi, arjunhar, jakhetia, chaganla, molisch}@usc.edu
†ESPOL Polytechnic University, Escuela Superior Politécnica del Litoral, ESPOL,
Facultad de Ingeniería en Electricidad y Computación, Km 30.5 vía Perimetral, P. O. Box 09-01-5863, Guayaquil, Ecuador

***Abstract*—Delay dispersion is one of the key propagation channel characteristics that impact system design and performance. In particular, for OFDM-based systems such as Wi-Fi, it determines both the amount of available frequency diversity and the minimum required cyclic prefix, which in turn impacts the spectral efficiency. For this reason, delay spread and power delay profiles have been analyzed for a long time. However, recent upgrades in Wi-Fi, in particular the addition of a new frequency range (6-7.1 GHz), and the introduction of adaptive beamforming, require a re-assessment based on new measurements. This paper presents extensive measurement results of RMS delay spread and interference quotient that take these developments into account. Results were measured in the 2.4-2.5, 5-6, and 6-7 GHz bands. Furthermore, we compare the "omni-directional" delay spread and interference quotient (i.e., when measured with omni-antennas at transmitter and receiver), to those that occur when beamformed antennas are used. We found that for both outdoor and indoor environments, beamforming typically improves the interference quotient (for a given window size) by about 3-5 dB. The 2.4 and 5-7 GHz bands show a significant difference, while we could not observe statistically significant differences between the 5-6 and 6-7 GHz bands.**

I. Introduction

Wireless Local Area Networks (WLANs) are one of the great success stories of the modern communication age, with an installed user base of billions of devices. Wi-Fi has become the dominant mode in which both computers and most smartphones are connected to the internet. In order to handle the concomitant increase in traffic load, the use of new frequency ranges, and new physical layer technologies are required. In terms of technology, recent versions of Wi-Fi are more heavily exploiting multiple antenna elements at both link ends, increasing the number of antenna elements that access points and end devices can have, as well as enabling multi-user MIMO. In terms of frequency range, an important step has been the recent approval of the 6-7 GHz band for Wi-Fi, more than doubling the available bandwidth.

In order to assess the impact of these developments and enable the design of new equipment that can efficiently exploit it, we first need to understand the propagation channel Wi-Fi devices operate in. *Channel sounding* allows us to measure the key parameters of a channel by application and processing of multidimensional spatio-temporal signals on the channel. Delay spread and the interference quotient are two key parameters in this regard. Delay spread provides an estimate of the delay dispersion, and thus the available frequency diversity, whereas the interference quotient is a window parameter that gives us a measure of the amount of energy we receive in a particular delay interval in comparison to the energy received outside it [1], and thus allows to assess and optimize the cyclic prefix (CP); insufficient CP may limit the channel data rates due to transmission errors that are caused by inter-symbol interference (ISI). The use of directional transmission (instead of the usual omni-directional) reduces the ISI, and/or allows for the design of shorter CPs, thus enhancing spectral efficiency (such directional transmission might be done with the explicit goal of reducing ISI, or might be incidential to other usage of beamforming). This stems from the simple fact that a directional beam at the receiver (RX), only accepts multipath signals that arrive within its illumination region (and similar at the transmitter (TX)). Reduction of Multipath Components (MPCs) generally reduces the delay spread as well, a fact that has been observed in a variety of frequency ranges and environments [2]–[6], though most of the recent emphasis has been on millimeter wave (mmWave) channels [7]–[10].

Specifically for Wi-Fi, we see that omni-directional antennas are widely used at both access point (AP) and user device (STA) in particular for low-cost devices, and will possibly coexist with the directional transmission systems that conform to the more recent versions. How both these systems impact key channel parameters is an important direction that has major implications of future Wi-Fi device design, in particular the possible reduction of CP to improve spectral efficiency. Therefore, this paper considers the comparison of directional and omni-directional delay spread and interference quotient. We specifically target all three Wi-Fi bands, 2.4, 5-6 and 6-7 GHz. The propagation characteristics in these channels are correlated but not identical. Moreover, the introduction of a new 6-7 GHz bandwidth has redefined these channels and to the best of our knowledge no previous study has covered this topic. The main contributions of this paper are: (i) experimental analysis of the new 6-7 GHz band and comparison to the existing Wi-Fi bands, (ii) comparison of *measured* rms delay spread and interference quotient between the case of omnidirectional antennas, beamforming at the AP,

and beamforming at the STA, in a variety of environments and (iii) discussion of the impact of the results on design of systems and standards. The rest of this paper is organized as follows. In Sec. II, we discuss our measurement setup and key parameter settings. We describe our measurement sites in Sec. III. Sec. IV highlights the major results for the current work. Finally, we conclude the manuscript in Sec. V.

II. Measurement Setup and Settings

A. Sounder Description

For our measurement campaign we used a frequency domain channel sounder based on a Vector Network Analyzer, VNA (Agilent model E5080A). The transmit signal from the VNA is amplified by a WENTEQ ABP1500-03-3730 power amplifier (PA), to a level of 29/27 dBm at the output (for 2.4/5-7 GHz respectively) and then transmitted from the TX antenna. On the other link end, the signal from the TX antenna goes through a bandpass filter in order to eliminate interference from adjacent bands, after which it is boosted by WENTEQ ABL0800-12-3315 LNAs (amplification 35/33 dB, noise figures 1.5/2 dB in 2.4/5-7 GHz band respectively) and sent through an RF cable (attenuation 9/15 dB/50ft) to port 2 of the VNA. Different settings of the VNA were chosen for the two bands, see Table I. Since the maximum measurable excess delay is determined by the subcarrier spacing, we aimed for similar such spacings in the two bands (though somewhat smaller in the 2.4 GHz band); yet due to the different available bandwidth this resulted in a much larger number of subcarriers in the 5-7 GHz band. The TX power was changed in order to get the maximum possible power from the PA. An IF bandwidth of 500 kHz for both bands was chosen as a compromise between measurement speed and noise power. Since the duration of a measurement sweep is larger than the typical channel coherence time in the presence of human movement, the setup can only be used under quasi-static conditions, which were ensured throughout our campaign.

TABLE I: VNA Settings

Band	**2.4 GHz**	**5-7 GHz**
Start Frequency	2.4 GHz	5 GHz
Stop Frequency	2.5 GHz	7 GHz
Number of Points	201	1601
Tx power	7 dBm	12 dBm

B. Antennas and directionality

Given the wide separation between the 2.4 and 5-7 GHz bands, we must use separate antennas for them. Furthermore, for our investigations of directional vs. omnidirectional spreads, we need directional (horn) as well as omnidirectional antennas. The omnidirectional antenna was model , which covers both bands. The COBHAM XPO2V-0.3-10.0/1381 antenna has a non-uniform beampattern in elevation, with a beamwidth

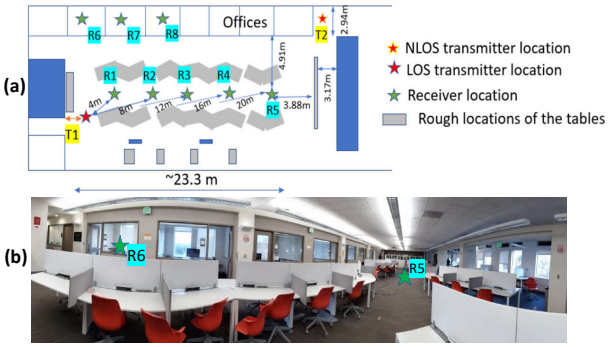

Fig. 1: (a) Diagram of the indoor open office environment. Two TX and eight RX locations. T1 is LOS and T2 is NLOS. (b) View from R1 to R5 and R6.

(full-width half-maximum, FWHM) of $\sim 90°$.[1] The directional antennas are a Cast Mini Reflector Grid Antenna (sold by L-com) for the 2.4-2.5 GHz with beam width of 12° in the E-Plane and 19° in the H-Plane, and 20dBi gain. For the 5GHz band, antennas from A-INFO with beam width ranging from 13° to 17° in E-plane and 16° to 19° for the H-Plane, and the gain ranges between 19 and 21 dB. The directional antennas were mounted on precision rotation stages from Diamond Engineering to point the main beam into different azimuths and elevations, and obtain the directional impulse responses [11]. Since a sweep of all combinations of TX and RX directions (full MIMO) would take more than 4 hours and thus greatly limit the number of locations that can be measured, we instead captured SIMO (omni antenna at the TX and horn at the RX) and MISO (vice versa) configurations. Equivalent SISO (omni at both link ends) channel characteristics are obtained through postprocessing, see Sec. IV.A.

III. Measurement Locations

A. Measurement Scenarios Description

We conducted measurement campaigns in two relevant environments: (i) an indoor open office environment and (ii) an outdoor courtyard; both are important in particular for enterprise WiFi. In the following, we describe the two environments and the measurement points.

1) Indoor Open Office Environment ("Leavey Library"): We conducted the measurement on the 2nd floor of the Leavey Library in the University of Southern California (USC). The floor has a wide studying area with small cubicles, chairs, and printers. On two sides of the open area, there are several small offices ($\sim$ 3.5m $\times$ 2.5m) with glass and wood doors to the open area. Inside the offices, there are tables, chairs, a whiteboard, and a computer monitor. The offices have glass windows to the outdoor area. In general, the floor structure and furniture resemble well modern open office environments. Fig. 3 shows the schematic diagram of the floor along with the TX and RX points.

[1]One limitation of our setup was the frequency variations of the gain of the omnidirectional antenna in the bands of interest (especially in the band of 5 -7 GHz), on the order of 6 to 8 dB, as well as deviations from a truly omnidirectional pattern of up to 4dB in azimuth. These variations in the pattern may have an impact in the results obtained in post-processing.

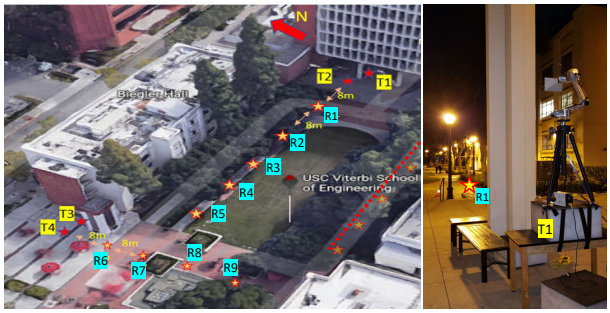

Fig. 2: (a) Viterbi Eng. Quad map with measurement locations. The measurement is done on three routes, each has one LOS and one NLOS Tx's. Route 1 and 3 have five Rx locations each (R1-R5) and (R10-R14), respectively, (Tx and Rx locations for route 3 are over the dotted line in the figure). Route 2 has four Rx locations (R6-R9). (b) Picture of T1 and R1 locations.

In total, we had two TX locations (one LOS and another NLOS), and eight Rx locations. The minimum distance was chosen to be four meters. The TX and RX antenna heights were 2.47m (.27m below the ceiling), and 1.55m, respectively.

2) Outdoor Courtyard Environment ("Viterbi Quad") : Outdoor measurements were performed in a quadrangle courtyard in front of Olin Hall of Engineering on the USC University Park Campus, Los Angeles. It is an L-shaped quadrilateral, as shown in Fig. 2. In one part of the courtyard, the measurement area is surrounded by trees, lampposts along its side, multi-story building with concrete walls and glass windows, and open grass. The second part has less vegetation with several tables, chairs and umbrellas, and a water fountain. We placed the TXs and RXs on paved ground.

In total, we measured with six TX and 14 RX locations and did the measurement along three routes. To emulate a typical outdoor hotspot, we elevated the TX antenna to 3m; the Rx antenna height is fixed at 1.55 m. The first route consists of five RX locations (R1-R5), with a NLOS and a LOS transmitter locations, T1 and T2, respectively. T1 is placed around 1.5 m behind a concrete base column (around 0.5 m wide) that blocks the LOS to R1-R5, Fig. 2. The second route has four RX locations (R6-R9) and two TX locations, T3 and T4, as NLOS and LOS, respectively. T2 is placed behind a building that blocks the LOS to R6-R9. We also performed measurement along a third route that mirrors the first one. In each route, the distance between the LOS TX and the closest RX is 8 m. Similarly, the distance between consecutive RXs is also 8 m, see Fig. 2.

IV. Results and Discussion

A. Data Processing

Given the scenarios previously described, we focus on computing the Delay Spread and Interference Quotient for the strongest beam direction and the omnidirectional reconstruction of the channel (See Fig 3). In our measurements we made one frequency sweep for every pointing direction of the horn antenna, where the pointing directions were spaced

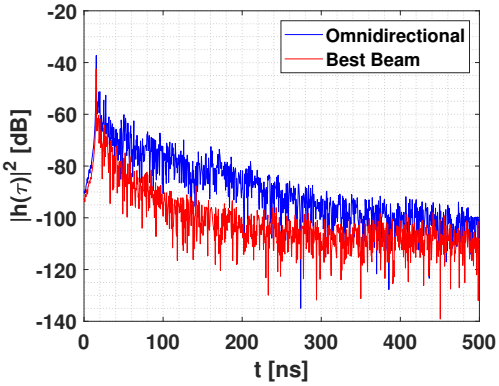

Fig. 3: Omnidirectional and Directional PDP

a 3-dB beamwidth of the antenna apart, i.e., 15^o for the 5 GHz band and 12^o for 2.4 GHz. This provides a collection of directional channel frequency responses for MISO and SIMO case. The impulse response from which we compute the directional parameters is obtained from the beam direction that provides the highest receive power

$$h_{\max}(f) = h(f, \theta_{\hat{i}}, \phi_{\hat{j}}); (\hat{i}, \hat{j}) = \arg\max_{i,j} |h(f, \theta_i, \phi_j)|^2 \quad (1)$$

To reconstruct the omnidirectional pattern from a MISO or SIMO capture we add all of the complex contributions together because the horn captures were done at steps equal to the Half Power Bandwidth (HPBW) of the antenna.

$$h_{\text{omni}} = \sum_i h(f, \theta_i, \phi_j) \quad (2)$$

Note that this omnidirectional reconstruction will not be perfect due to the non-ideal behavior of the horn antennas, leading to some residual ripples. Using the thus-defined directional and omnidirectional channel frequency responses shown calculate the root mean square Delay Spread and Interference Quotient as follows:

1) We compute the power delay profile (PDP) by

$$h_k(\tau) = \mathcal{F}^{-1}\left(h_k(f)\right) \quad (3)$$

$$P_k(\tau) = |h_k(\tau)|^2 \quad (4)$$

where $\mathcal{F}^{-1}$ is the Inverse Fast Fourier Transform (IFFT) and k can be max for the strongest beam direction or $omni$ for the omnidirectional response.

2) We next apply a delay gating and noise thresholding to the PDP, in order to eliminate the wrap-around effect of the IFFT and noise values of the realization:

$$P_{calc}(\tau) = [P_k(\tau) : (\tau \leq \tau_{gate}) \wedge (P_k(\tau) \geq P_\lambda)] \quad (5)$$

and 0 if it does not fulfill these conditions. Here τ_{gate} is the delay gating value and P_λ is the noise threshold, where τ_{gate} is set to 500 ns and for P_λ we set the value to be 6dB above the noise floor of the PDP.

3) After that, the delay spread is calculated as the second central moment of the PDP [1].

4) For the calculation of the Interference Quotient, the computation is done as follows [1]:

$$Q_T = \max_{\tau_0:\tau_0 \leq \tau_{gate}} \frac{\sum_{\tau=\tau_0}^{\tau_0+T} P_{calc}(\tau)}{P_m - \sum_{\tau=\tau_0}^{\tau_0+T} P_{calc}(\tau)} \quad (6)$$

Q_T is a Signal to Interference Ratio (SIR) measure of the ISI in the scenario, A higher value of Q_T indicates that the ISI effect is small. Note that the Q_T and σ_τ are both measures for the amount of delay dispersion, but they are essentially different. The Q_T incorporates a "threshold effect": any MPC within the window is useful, any MPC outside it is interference; it is thus a good measure for systems with finite-length equalizers and OFDM with CP, but it depends on the considered window size T. The rms delay spread, on the other hand, weights MPCs quadratically with their offset from the mean delay; it can be related (via an uncertainty relationship) to the coherence bandwidth, and thus serves as a measure for the available frequency diversity. Note that different PDPs can have the same rms delay spread.

The procedure explained before will be used to analyze the 2.4-2.5 and 5-6 and 6-7 GHz Wi-Fi bands. The first investigation was a comparison of the 5-6 and 6-7 GHz bands, which is especially interesting as the 6-7 GHz band has been opened to WiFi usage only in 2019 [12], and thus has hardly been explored. However, our comparisons (shown here) did not identify any statistically significant differences in the delay dispersion parameters between those bands. Thus one important conclusion from our analysis is that the many results available for the 5-6 GHz band seem to apply to the 6-7 GHz band as well While this conclusion might seem unsurprising given the close proximity of those two bands, it is for the first time (to our knowledge) that it has been verified experimentally in the considered environments. Due to the strong similarity between 5-6 and 6-7 GHz, we treat it as a single band in the remainder of this paper, in order to not overload the figures and results. Furthermore, in order to make a fair comparison between the 2.4 and the 5-7 GHz band, a sliding window approach will be used for both to measure and analyze the results. The sliding window values used for this case will be 20, 40, and 80 MHz. For the calculation of Q_T we will use different values of T related to cyclic prefix duration used for Wi-Fi systems and integer fractions of those values (e.g 25, 50, 100, 200 and 400 nanoseconds).

B. Delay Spread

From physical considerations, we anticipate that the reduction in delay spread when using directional antennas is stronger if the directional antennas are applied at the link end with the larger angular dispersion. In our setting, this lets us anticipate that the SIMO configuration (i.e., the directional antenna is at the link end with the 1.55 m height) will show a smaller directional delay spread than the MISO configuration (where the directional antenna is at the link end that is more elevated, i.e., the AP). From the plots in Fig. 4, we

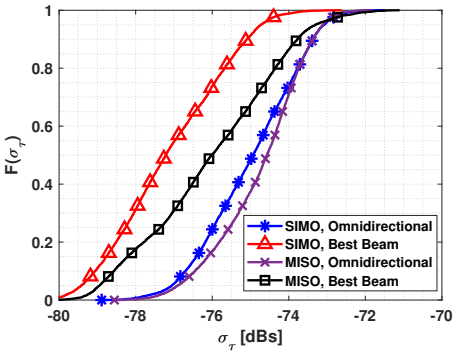

(a) LOS

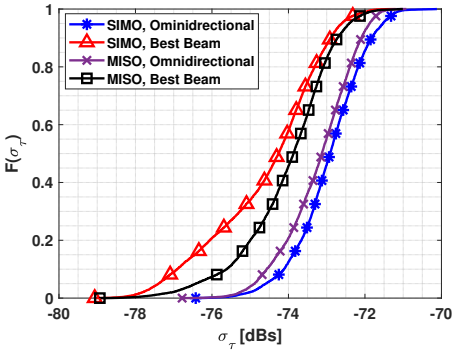

(b) NLOS

Fig. 4: Delay Spread for 5GHz band, Leavey Library, SW = 80MHz.

can see that this is indeed what we observe.[2] This physical effect is enhanced in LOS scenarios were the concentration of strong MPCs is high compared with NLOS were MPCs are more spread in the delay domain. This effect can be observed by comparing the curves in Fig 4(a) and Fig 4(b) were the difference in median values between the directional and omnidirectional cases ($\sigma_\tau^{50\%}$) is approximately 3 dB. For the MISO/LOS case the difference is reduced to 2 dB. For the NLOS case, the difference is reduced to 2dB as expected. Note that the curves show the cumulative distribution function of the delay spread, where the considered ensemble includes the different small-scale fading realizations corresponding to the sliding window positions, as well as the different measurement locations. Furthermore, note that we represent the delay spread on a dBs scale, i.e., the linear delay spread is $10^{x/10}$, where σ_τ; for example, -70 dBs corresponds to 100 ns; this representation is common in the channel modeling literature.

For the outdoor scenario we anticipate higher number of MPCs and longer detours of reflected MPCs. Therefore, for the LOS case, large differences between the omnidirectional

[2]Note that the "omnidirectional spread" for the SIMO and the MISO case should be similar, but not identical, because we are using two different "omnidirectional" antennas at the link ends: an actual dipole antenna on one link end, and the reconstructed (from the various horn positions) omni-antenna at the other link end. These two antennas are both (approximately) omnidirectional in azimuth, but have different elevation patterns. Thus, when we switch those antennas between TX and RX, the delay spread will change somewhat.

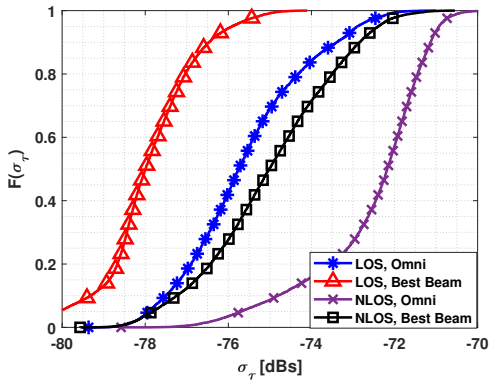

Fig. 5: Delay Spread for Viterbi Quad, MISO Case, SW = 80MHz.

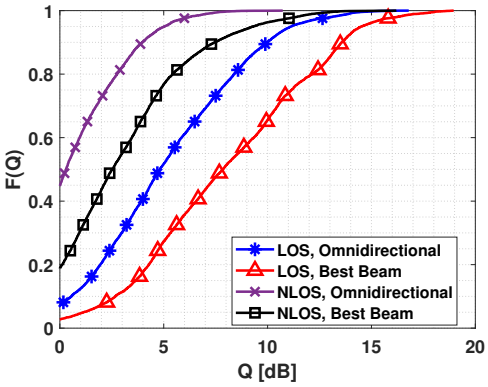

Fig. 6: Interference Quotient for Leavey Library MISO Case, T=25ns, SW = 80MHz.

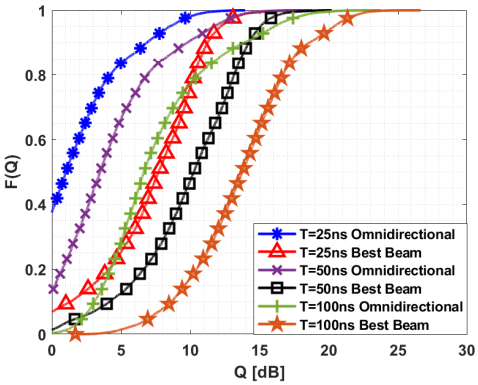

Fig. 7: Interference Quotient for Viterbi Quad MISO NLOS Case, SW = 80MHz.

and directional σ_τ values can be expected.

For the outdoor NLOS scenario, the routes consisted in moving the TX out of the LOS of the RX and be blocked by a pillar in Route 1 and blocked by a building edge in Route 2. We focus here on the MISO case which corresponds to directionality (beamforming) at the AP side in our setup. In Fig.5 we can see that the difference between the omnidirectional and directional cases for LOS and NLOS are very similar, between 2 and 3dB for both LOS and NLOS cases.

As final comparison the same analysis was done for 2.4 GHz band with the same sliding windows. We expect somewhat larger delay spreads (both for the omni-directional and the directional case), due to the different dynamic range of the setups in the two cases. In Table II, mean value for Delay Spread calculated for the 2.4 and 5GHz band using 20, 40 and 80 MHz sliding windows are shown, confirming this conjecture. Furthermore, the difference between directional and omni-directional spreads for 2.4 GHz is approximately 1 dB compared to differences up to 3dB for the 5GHz band cases.

C. Interference Quotient

For the analysis of the Interference Quotient focus we again concentrate on the MISO case due to its practical importance. We anticipated that Q_T values for omnidirectional cases will be smaller compared to the directional values, given that the delay spread is reduced for the directional case. As can be seen from Fig. 6 the Q_T is less than 5dB in 50% of cases for omnidirectional, but only in 25% of cases in the directional case for LOS. This fact indicates the reduction of self interference by using beamforming/beams at the Tx side. Additionally, for the NLOS case there is an improvement of 3dB in average compared to the omnidirectional case.

Future communication systems are planned to use reduced cyclic prefix [12]. Given this fact, for the outdoor scenario analysis the focus was to test different values of T (CP length) and analyze its effect on Q_T. Reduction of the duration of T significantly decreases Q_T but that effect can be compensated to some extent by beamforming. This effect can be seen in Fig. 7, by reducing T, we observed a 50% reduction in median of the Q_T from a 100 ns window to a 50 ns and a 90% reduction if we reduce it to 25 ns. However, by using a directional beam we can have similar values using $T = 25ns$ than an omnidirectional case using $T = 100ns$. It is important to mention that the values shown before correspond to a NLOS scenario were the MPC dispersion is higher. This effect can be exploited in future Wi-Fi communication systems that plan to use smaller Cyclic Prefix and beamforming to improve performance and Quality of Service. We present in Table III the median values of Q_T using different values of T for 2.4 GHz and 5-7 GHz bands, showing similar effects for a variety of environments and frequency bands.

V. Conclusion

In this document we presented measurements of the delay dispersion (σ_τ and Q_T) of Wi-Fi with omnidirectional and directional antennas in different bands. We firstly measured that the characteristics in the new 6-7 GHz band are not significantly different from the previously explored 5 GHz band. Furthermore, our results showed that directional delay spreads are smaller, and interference quotients larger, compared to the omndirectional ones. Consistent with physical considerations of the scenario, it was identified that SIMO configuration showed smaller values of delay spread compared to MISO, especially in NLOS scenarios. Considering outdoor scenarios with multiple MPCs we observed that beamforming can compensate (i.e., keep Q_T constant) a reduction of the CP,

TABLE II: Mean Delay Spread values in dB for different configurations of sliding windows.

		2.4 GHz			5 GHz		
		20 M	**40 M**	**80 M**	**20 M**	**40 M**	**80 M**
OMNI Leavey Library	**SIMO LOS**	-73.54	-74.26	-74.61	-73.95	-74.53	-74.99
	SIMO NLOS	-72.25	-72.74	-72.94	-72.43	-72.72	-72.95
	MISO LOS	-73.42	-74	-74.38	-73.84	-74.35	-74.76
	MISO NLOS	-72.44	-72.92	-73.17	-72.70	-72.99	-73.23
OMNI Viterbi Quad	**SIMO LOS**	-72.90	-73.12	-74.16	-74.15	-74.62	-75.3
	SIMO NLOS	-71.63	-72.08	-72.25	-71.96	-72.28	-72.49
	MISO LOS	-73.1	-73.33	-74.35	-74.37	-74.85	-75.61
	MISO NLOS	-71.86	-72.33	-72.49	-72.02	-72.39	-72.56
Best Beam Leavey Library	**SIMO LOS**	-74.51	-75.6	-76.55	-75.15	-76.39	-77.12
	SIMO NLOS	-73.37	-74.02	-74.56	-73.70	-74.12	-74.6
	MISO LOS	-74.16	-75.18	-75.67	-74.57	-75.42	-76.03
	MISO NLOS	-72.61	-73.17	-73.56	-73.27	-73.65	-74.06
Best Beam Viterbi Quad	**SIMO LOS**	-73.98	-74.2	-76.66	-75.7	-76.31	-77.68
	SIMO NLOS	-73.56	-74.97	-75.52	-74.06	-75	-75.6
	MISO LOS	-74.25	-74.39	-77.34	-75.78	-76.36	-77.93
	MISO NLOS	-73.68	-75.12	-75.39	-73.86	-74.62	-75.01

TABLE III: Median Interference Quotient in dB for different T values*, SW = 80MHz.

		2.4 GHz					5 GHz				
		25 ns	**50 ns**	**100 ns**	**200 ns**	**400 ns**	**25 ns**	**50 ns**	**100 ns**	**200 ns**	**400 ns**
OMNI Leavey Library	**SIMO LOS**	6.26	8.47	12.9	20.49	32.75	5.67	8.89	13.61	22.20	∞
	SIMO NLOS	-1.09	2.25	7.88	15.62	27.85	0.07	2.94	7.74	15.31	30.62
	MISO LOS	5.86	8.34	12.19	20.89	33.06	4.81	8.11	12.98	20.76	∞
	MISO NLOS	1.77	4.4	7.9	16.53	28.95	0.29	3.44	8.59	16.14	31.54
OMNI Viterbi Quad	**SIMO LOS**	8.27	11.22	14.08	19.12	29.24	8.55	10.83	14.42	20.29	33.65
	SIMO NLOS	1.13	3.37	7.35	13.21	23.74	1.74	4.13	7.19	13.79	26.83
	MISO LOS	7.68	11.39	14.61	18.94	28.55	8.73	11.43	15.05	21.03	37.13
	MISO NLOS	1.77	4.44	7.33	13.13	24.99	1.03	3.49	6.64	13.7	27.56
Best Beam Leavey Library	**SIMO LOS**	10.04	12.95	17.73	23.43	33.3	9.41	12.98	18.86	29.13	∞
	SIMO NLOS	6.02	8.35	11.52	18.85	29.93	3.67	7.11	11.91	18.82	35.83
	MISO LOS	9.32	11.97	15.78	22.53	33.04	7.85	11.11	15.83	25.04	∞
	MISO NLOS	2.26	4.86	10.57	16.15	28.77	2.53	5.96	10.92	18.18	33.43
Best Beam Viterbi Quad	**SIMO LOS**	12.71	15.03	19.74	23.73	31.6	10.88	14.22	19.02	26.47	∞
	SIMO NLOS	9.17	12.54	16.18	21.16	29.45	7.26	10.6	15.01	20.64	32.31
	MISO LOS	12.94	15.12	19.26	24.44	33.94	10.51	14.15	18.08	27.26	∞
	MISO NLOS	9.1	11.93	15.2	20.11	29.54	7.71	10.25	13.76	19.04	31.08

*Values equal to ∞ indicate that T is large enough to eliminate completely the self interference created by the scenario.

which indicates that spectral efficiency can be improved without compromising performance by using directional beams rather than omnidirectional antennas.

Acknowledgement: The authors thank Z. Cheng, P. Koivumaki, H. Hammoud, F. Rottenberg and T. Choi for their help with the measurements. The financial support from a gift by Cisco is gratefully acknowledged. J. Gomez-Ponce research work is partially supported by the Foreign Fulbright Ecuador SENESCYT Program.

REFERENCES

[1] A. F. Molisch, *Wireless communications*. Wiley, 2011.

[2] H. Yang, M. H. Herben, I. J. Akkermans, and P. F. Smulders, "Impact analysis of directional antennas and multiantenna beamformers on radio transmission," *IEEE Trans. on vehic. tech.*, vol. 57, no. 3, pp. 1695–1707, 2008.

[3] A. Simonsson, H. Asplund, J. Medbo, and K. Werner, "Beamforming impact on time dispersion assessed on measured channels," in *2018 IEEE 87th Vehic. Technology Conf. (VTC Spring)*, 2018, pp. 1–6.

[4] A. Hammoudeh and D. Scammell, "Effect of receive antenna directivity on rms delay spread and coherence bandwidth for indoor millimetre wave mobile radio channels," in *2003 5th European Personal Mobile Comm. Conf. (Conf. Publ. No. 492)*, 2003, pp. 406–411.

[5] J. A. Dabin, Nan Ni, A. M. Haimovich, E. Niver, and H. Grebel, "The effects of antenna directivity on path loss and multipath propagation in uwb indoor wireless channels," in *IEEE Conf. on Ultra Wideband Systems and Technologies, 2003*, 2003, pp. 305–309.

[6] M. Pettersen, P. Lehne, J. Noll, O. Rostbakken, E. Antonsen, and R. Eckhoff, "Characterisation of the directional wideband radio channel in urban and suburban areas," in *Gateway to 21st Century Communications Village. VTC 1999-Fall. IEEE VTS 50th Vehicular Technology Conference (Cat. No. 99CH36324)*, vol. 3. IEEE, 1999, pp. 1454–1459.

[7] M. Kim, J. Liang, H. Kwon, and J. Lee, "Directional delay spread characteristics based on indoor channel measurements at 28ghz," in *2015 IEEE 26th Annual Intern. Symp. on Personal, Indoor, and Mobile Radio Communications (PIMRC)*, 2015, pp. 403–407.

[8] G. R. MacCartney, M. K. Samimi, and T. S. Rappaport, "Exploiting directionality for millimeter-wave wireless system improvement," in *2015 IEEE intern.l conf. on comm. (ICC)*. IEEE, 2015, pp. 2416–2422.

[9] M.-D. Kim, J. Liang, J. Lee, J. Park, and B. Park, "Directional multipath propagation characteristics based on 28ghz outdoor channel measurements," in *2016 10th European Conf. on Antennas and Propagation (EuCAP)*. IEEE, 2016, pp. 1–5.

[10] G. R. Maccartney, T. S. Rappaport, S. Sun, and S. Deng, "Indoor office wideband millimeter-wave propagation measurements and channel models at 28 and 73 ghz for ultra-dense 5g wireless networks," *IEEE access*, vol. 3, pp. 2388–2424, 2015.

[11] M. Steinbauer, A. F. Molisch, and E. Bonek, "The double-directional radio channel," *IEEE Antennas and Prop. Mag.*, vol. 43, no. 4, pp. 51–63, Aug 2001.

[12] E. Khorov, I. Levitsky, and I. F. Akyildiz, "Current status and directions of ieee 802.11be, the future wi-fi 7," *IEEE Access*, pp. 1–1, 2020.